ELSEVIER

Carbohydrate Research 261 (1994) 91–102

CARBOHYDRATE RESEARCH

Conformational analysis of ester and ether linkages in lignin–arabinoxylan complexes †

Frantisek Bízik [a], Igor Tvaroska [a,*], Milan Remko [b]

[a] *Institute of Chemistry, Slovak Academy of Sciences, 842 38 Bratislava, Slovak Republic*
[b] *Department of Pharmaceutical Chemistry, Comenius University, 832 32 Bratislava, Slovak Republic*

(Received December 11th, 1992; accepted in revised form March 1st, 1994)

Abstract

Conformational flexibility around the ester and ether linkages in 5-*O*-cinnamoyl-α-L-arabinofuranose (**1**) and 5-*O*-[(*S*)-1-phenethyl]-α-L-arabinofuranose (**2**), models for lignin–carbohydrate complexes, has been investigated by molecular orbital PCILO calculations. The structures of individual minima were refined by minimising the energy by adjusting geometrical parameters from the distinct low-energy regions in two-dimensional maps. The calculations show that the ester and ether linkages in lignin–carbohydrate complex models display a large amount of conformational freedom. This involves a rapid equilibrium between the various pseudorotamers of the furanose ring, rotamers of the exocyclic group, and rotation around the ester and ether linkages. The calculations reveal the strong influence of solvent on the conformer populations and that this effect is more pronounced in the ether linkage. The results for aqueous solution predict that (*a*) the North- and South-type pseudorotamers of the α-L-arabinofuranose ring are present in equilibrium in approximately equal amounts in the ester **1**, whereas the North-type pseudorotamers prevail in the ether **2**; (*b*) the *gt* conformation is more populated in both compounds; and (*c*) the antiperiplanar orientation is dominant in both the ester and ether. The present results give some insight into the conformational flexibility that both molecules display, shed light on the possible arrangement of hydrophilic and hydrophobic parts of lignin–carbohydrate complexes, and provide the basis for the generation of more accurate models for further studies of lignin–carbohydrate complexes.

† Presented at the XVIth International Carbohydrate Symposium, Paris, France, July 5–10, 1992.

* Corresponding author. Present address: Centre de Recherches sur les Macromolécules Végétales, CNRS, BP 53 X, 38041 Grenoble Cedex, France.

SSDI 0008-6215(94)00090-3

1. Introduction

The existence of a covalent linkage between lignin and saccharides remained speculative for several decades. The difficulty of the experimental determination of such a linkage came from the fact that, in most cases, drastic conditions have to be employed in order to achieve the isolation of a lignin–carbohydrate complex (LCC) from the cell wall. As a result of many experiments, several oxygen bonds which connect lignin to the saccharide part of the cell wall were discovered [1–8], namely glycosidic linkages, ester linkages, and ether bonds. From experimental studies of various plants [9], it is well known that plants which are different in their evolution (softwoods, hardwoods, graminaceous plants) contain structurally different molecular species of hemicellulose and lignin. This implies the existence of variations in the saccharide linkage to lignin in different type of plants. The isolated lignin–carbohydrate complexes were studied by means of various physicochemical methods [10–13] in order to obtain more information about the nature of those bonds. However, the molecular structure of LCC is still not known.

In the light of the known limitations in the experimental investigation of the molecular structure of LCC, we carried out, in our previous study [14], the conformational analysis of benzyl ether and benzyl ester linkages in lignin–glucopyranose complexes. In order to learn more about the likely conformations in ester and ether linkages found in lignin–carbohydrate complexes, we have modelled here the conformational properties of the lignin and arabinofuranose parts of LCC in various solvents.

2. Methods

For the study of the conformational properties of the ester and ether linkage in a lignin–carbohydrate complex, 5-*O*-cinnamoyl-α-L-arabinofuranose (**1**) and 5-*O*-[(*S*)-1-phenethyl]-α-L-arabinofuranose (**2**) were chosen as models (Scheme 1). The relative orientation of the lignin and saccharide parts of LCC linked by the ester and ether linkage is given by the torsional angles: ω = O-4–C-4–C-5–O-5, Ψ = C-4–C-5–O-5–C-6, and χ = C-5–O-5–C-6–C-7. For **1**, the more stable antiperiplanar arrangement [15] of the cinnamoyl moiety was considered.

The analysis of **1** and **2** was started by creating two-dimensional conformational energy (Ψ, ω) maps, calculated in 20° intervals using the PCILO quantum chemical method [16]. The PCILO method was chosen primarily because it has been shown to be suitable for modelling conformational properties of the glycosidic linkage [17]. Local minima on the (Ψ, ω) maps were used for further investigation. When analysing arabinofuranose conformations, it should be recognised that a five-membered ring is more flexible than a pyranose ring. The five-membered furanose ring is generally nonplanar. It can be puckered in an envelope (*E*) form with four atoms in a plane and the fifth atom out, or in a twist (*T*) form with two adjacent atoms displaced on opposite sides of a plane through the other three atoms. All the possible conformations of the furanose ring can be

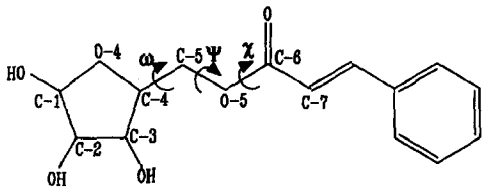

1

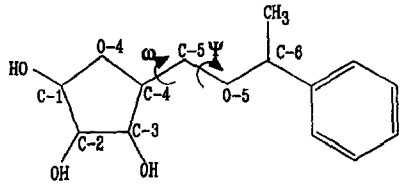

2

Scheme 1.

systematically related by the use of the pseudorotational wheel. The position on the wheel is described [18] by the angle of pseudorotation ϕ_2 and puckering amplitude q, and corresponds to one of the furanose ring conformations. It is useful to describe these structures with the convenient North-South (N-S) descriptors. Thus, for the α-L-arabinofuranosyl ring, two classes of conformers can be distinguished: the North-type (N, the angle of pseudorotation $-90° < \phi_2 < +90°$) and the South-type (S, $+90° < \phi_2 < 270°$). Conversion between the various forms is thought to occur usually through pseudorotation. Therefore, to take into account the furanose ring flexibility, two rings were built for each of the local minima on the (Ψ, ω) potential surface. For this purpose, we selected one South- and one North-type conformer on the pseudorotation wheel, which were assumed in the conformational analysis of the arabinofuranose ring in solution [19]. Starting bond lengths and angles were taken from crystallographic data [20–23] and the structure of each conformation was fully optimised. During optimisation, all the internal coordinates were allowed to vary and the required accuracy was 0.1 pm for bond lengths, 0.05° for bond angles, and 0.5° for torsion angles. The method for calculation of the solvent effect on conformer stability has been described in detail in our previous papers [24,25]. The contributions of the solvent effect were calculated for each conformer of **1** and **2**.

3. Results and discussion

Conformational energy (Ψ, ω) maps. — The potential energy (Ψ, ω) maps for the isolated molecule and for aqueous solutions of **1** and **2** are shown in Figs. 1 and 2. For **2**, the orientation of the third torsional angle χ was antiperiplanar. We chose this orientation because, in the other two staggered conformations ($\chi = +60°$

or −60°), energies were always higher due to steric interactions. The potential energy surfaces computed for both types of linkage are comparable. There is the main low-energy domain centred at $\Psi = 180°$ which spans over 360°, along with three well-defined low-energy domains for the ω torsion angle. In the antiperiplanar orientation ($\Psi = 180°$), bulky terminal groups (five-membered ring and substituted phenyl derivatives) in both molecules are so far distant that the compounds have reasonable potential energy. In agreement with this, a rotational flexibility of **2** is more hindered in comparison with that of **1**, especially in the −synclinal orientation ($\Psi = -60°$). This might be explained by stronger steric interactions between the furanose ring and methyl group in **2** than between the furanose ring and the oxygen of the carbonyl group in **1**. On the other hand, a clear similarity in symmetry of maps for both compounds is evident. Three distinct low-energy domains about ω are consistent with *gauche–gauche* ($\omega = -60°$, *gg*), *gauche–trans* ($\omega = 60°$, *gt*), and *trans–gauche* ($\omega = 180°$, *tg*) orientations about the C-4–C-5 bond. In both molecules, the lowest energy area is centred on $\omega = 60°$. The preference for this orientation is in agreement with the *gauche* effect in the O–C–C–O segment of atoms [26]. The results shown in Figs. 1 and 2 indicate barriers of 10–15 kJ/mol for reorientations of the exocyclic groups, and that transitions are most easily accomplished when the bulky terminal groups are oriented in the antiperiplanar position. These maps further illustrate that energy rises more sharply with changing Ψ than ω. The relative energies of the remaining regions are considerably higher, and conformational transitions to these regions require more than 20 kJ/mol.

Comparison of the conformational energy (Ψ, ω) maps in Figs. 1 and 2 shows

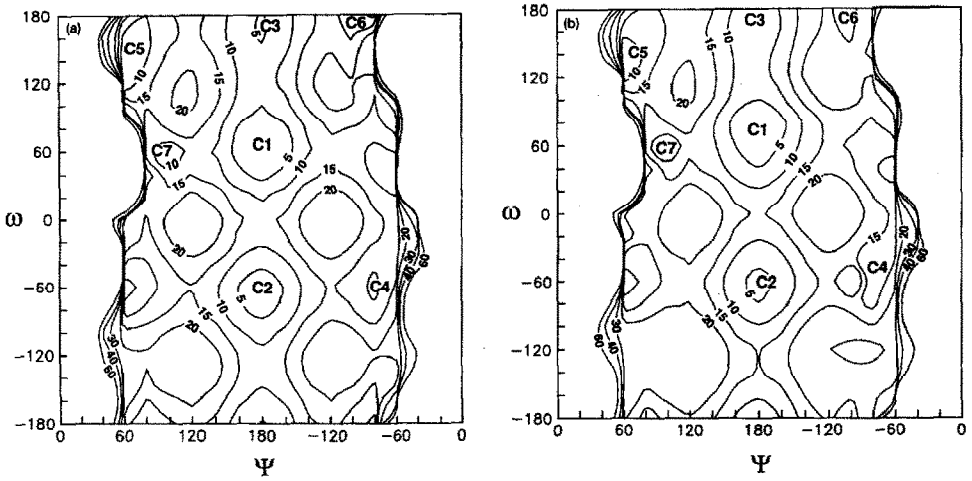

Fig. 1. PCILO potential energy surfaces of 5-*O*-cinnamoyl-α-L-arabinofuranose (**1**) calculated for the isolated molecule (a) and aqueous solution (b). Isoenergy contours are drawn for 4, 8, 12, 20, 30, and 60 kJ/mol energy levels above the minimum in each map. The locations of the stable minima (C1–C7) are indicated on the maps.

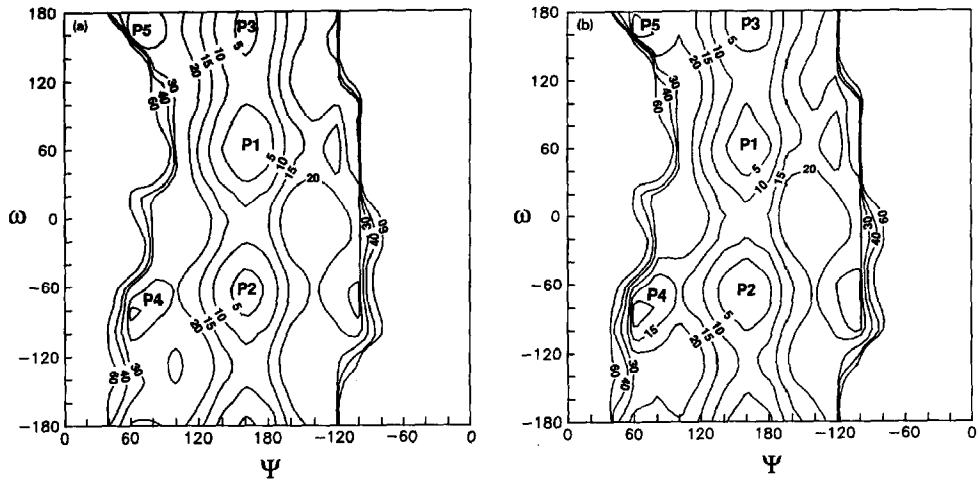

Fig. 2. PCILO potential energy surfaces of 5-*O*-[(*S*)-1-phenethyl]-α-L-arabinofuranose (**2**) calculated for the isolated molecule (a) and aqueous solution (b). Isoenergy contours are drawn for 4, 8, 12, 20, 30, and 60 kJ/mol energy levels above the minimum in each map. The locations of the stable minima (P1–P5) are indicated on the maps.

only a relatively small alteration of the character of the maps as a result of the change of solvent. The conformational energy maps of **1** and **2** in solution preserve the shape of the maps observed for isolated molecules. The solvent effect manifests itself mainly in the change of energies of individual conformers. However, the quantitative character of the change is different in both molecules and will be discussed next. The survey of the calculated (Ψ, ω) potential energy surfaces revealed the existence of 10 low-energy regions for **1** and 7 regions for **2**.

Description of minima. — In order to understand how the orientations at C-4 and C-5 influence the conformations of the α-L-arabinofuranose ring, North- and South-type rings were built for each of the 17 low-energy regions and these 34 conformers were used as starting points for the PCILO energy minimisation by relaxation of the internal geometrical parameters. For **1**, nine of the 20 initial conformations converged to the one from already found minima. For **2**, a similar behaviour was observed, with three minima converging towards the same minimum. As a result, 11 conformers corresponding to seven (Ψ, ω) local minima (C1–C7) were found for **1**. For **2**, seven conformers corresponding to five (Ψ, ω) local minima (P1–P5) were calculated. The minimisation of the lowest energy conformations, C1 and P1 ($\Psi = 180°$, $\omega = 60°$), converges for both compounds into two ring pseudorotamers. They are localised in N and S regions of the pseudorotational wheel and lie within a 2.5 kJ/mol energy interval. Among 11 minima considered for **1**, three belong to the North domain and eight to the South domain. In the case of **2**, two belong to the North domain and five to the South domain. The linkage torsion angles and puckering parameters from the resulting minima are listed in Tables 1 and 2.

To compare the five-membered ring structures calculated with the experimental

Table 1
PCILO calculated relative energies (kJ/mol), torsion angles (degrees), and puckering parameters for the stable conformers of 5-*O*-cinnamoyl-α-L-arabinofuranose (1)

Conformer	ΔE	Ψ	ω	ϕ_2	q (Å)
C1–N	0.0	180.8	65.9	268.6	0.28
C1–S	0.38	181.1	67.0	107.5	0.22
C2–S	1.76	179.5	304.1	105.7	0.22
C3–S	2.81	178.9	178.8	106.8	0.22
C3–N	12.60	178.7	181.8	251.1	0.38
C4–S	4.77	286.1	309.1	108.7	0.22
C5–S	9.71	59.7	152.0	126.8	0.27
C6–S	11.14	289.4	182.3	124.1	0.29
C6–N	16.12	282.8	160.9	306.9	0.20
C7–S	11.85	65.6	86.2	135.9	0.27
C7–N	13.19	82.9	55.8	271.2	0.24

data for compounds possessing an arabinofuranose ring, the geometries of all available relevant structures were retrieved from the Cambridge Structural Database. From 25 different crystal structures of arabinofuranosides, only four compounds carrying a carbon substituent at C-1 were retrieved. The structures and their reference codes are as follows. DOJBEJ: 4-(α-D-arabinofuranosyl)-imidazo(4,5-*c*)-4,5,6,7-tetrahydropyridine [20]; DOJBIN: 1(*S*)-(α-D-arabinofuranosyl)-1,2,3,4-tetrahydro-β-carboline [21]; CXBARF: 5-*O*-benzoyl-1-carbamoyl-1-deoxy-α-D-arabinofuranose [22] [*C*-(5-*O*-benzoyl-α-D-arabinofuranosyl)formamide]; GAPCUV: 2-β-D-arabinofuranosylthiazole-4-carboxamide [23]. Their puckering parameters (q, ϕ_2) are DOJBEJ = (0.354 Å, 278.1°), DOJBIN = (0.364 Å, 177.7°), CXBARF = (0.338 Å, 75.1°), and GAPCUV = (0.401 Å, 53.5°). It is interesting that among the four structures considered, three belong to the South domain and one to the North domain, whereas out of the remaining 21 different arabinofuranose rings, 13 forms crystallise in an N domain and 8 in an S domain. This suggests an important role of the substituents at C-1.

The five-membered ring in the crystal structure of DOJBEJ adopts a $^3T_2$ conformation with $\phi_2 = 278.1°$. Three calculated minima are located in the corre-

Table 2
PCILO calculated relative energies (kJ/mol), torsion angles (degrees) and puckering parameters for the stable conformers of 5-*O*-[(*S*)-1-phenethyl]-α-L-arabinofuranose (2)

Conformer	ΔE	Ψ	ω	ϕ_2	q (Å)
P1–N	0.0	178.8	66.0	273.9	0.27
P1–S	2.47	186.9	67.9	125.3	0.23
P2–S	4.86	183.9	304.6	113.1	0.23
P3–S	5.65	169.7	176.7	109.3	0.22
P3–N	11.43	185.4	184.7	171.3	0.19
P4–S	6.57	81.9	295.6	109.5	0.23
P5–S	9.09	63.2	165.9	112.4	0.23

Table 3
Calculated molar fractions for the stable conformers of 5-*O*-cinnamoyl-α-L-arabinofuranose (**1**) in a vacuum and in solution

Conformer	Vacuum	1,4-Dioxane	Chloroform	Methanol	Me_2SO	Water
C1–N	34.82	38.27	39.05	43.22	43.46	52.07
C1–S	29.93	28.72	28.33	26.93	27.54	22.38
C2–S	17.13	14.86	14.91	13.25	12.04	11.01
C3–S	11.23	10.97	10.46	9.29	9.67	6.98
C3–N	0.22	0.20	0.19	0.18	0.19	0.13
C4–S	5.08	5.58	5.60	5.60	5.63	5.60
C5–S	0.69	0.77	0.79	0.80	0.79	0.84
C6–S	0.39	0.02	0.05	0.01	0.0	0.01
C6–N	0.05	0.0	0.0	0.0	0.0	0.0
C7–S	0.29	0.41	0.44	0.54	0.50	0.84
C7–N	0.17	0.18	0.18	0.17	0.18	0.14

sponding "classical" N region between the ${}_2E$ and ${}^3E$ pseudorotamers with ϕ_2 ranging from 252° to 288°. These conformers (Tables 1 and 2) are C1-N and C7-N of **1** and P1-N of **2**. Among them are the most stable conformers of **1** and **2**, namely C1-N and P1-N. Such an agreement between theoretical conformers and observed crystal structure supports the results of modelling the stereochemistry of LCC. The structure of the P3-N conformer is close to the structure of DOJBIN.

Conformational equilibrium. — The calculated results imply that a rapid interconversion can occur which involves rotamers about the C-4–C-5 bond and pseudorotation of the ring. The relative populations of these rotamers depend on the solvent and the substituents at O-5. Molar fractions of stable conformers estimated from calculated values of the free energy differences, using the Boltzmann distribution, are given in Tables 3 and 4. Molecular drawings associated with the three most populated conformers of **1** and **2** in aqueous solution are shown in Figs. 3 and 4.

For **1** in a vacuum, the stability of (Ψ,ω) conformers decreases in the order C1 > C2 > C3 > C4 > C5 > C6 > C7. Three conformers are dominant in the equilibrium mixture, namely C1, C2, and C3. The population of the C2 and C3

Table 4
Calculated molar fractions for the stable conformers of 5-*O*-[(*S*)-1-phenethyl]-α-L-arabinofuranose (**2**) in a vacuum and in solution

Conformer	Vacuum	1,4 Dioxane	Chloroform	Methanol	Me_2SO	Water
P1–N	58.19	60.73	63.61	73.22	71.44	85.24
P1–S	21.48	15.99	14.64	9.33	9.90	3.27
P2–S	8.20	8.71	7.83	5.72	6.38	2.72
P3–S	5.95	6.87	6.40	4.99	5.39	2.91
P3–N	0.58	0.69	0.71	0.74	0.69	0.82
P4–S	4.11	5.34	5.31	4.91	4.95	4.51
P5–S	1.49	1.66	1.50	1.09	1.24	0.53

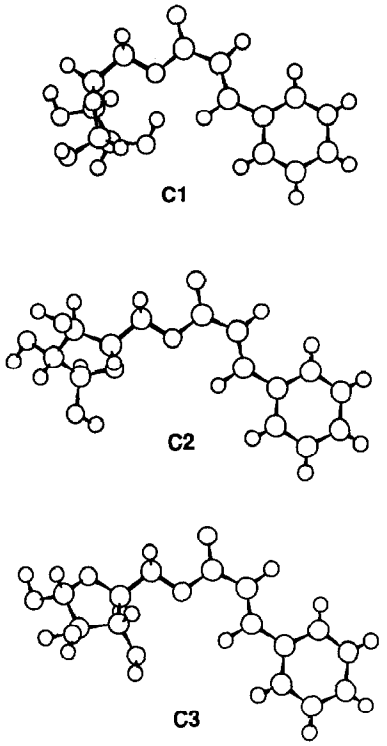

Fig. 3. Molecular representation of the three lowest energy conformations of 5-*O*-cinnamoyl-α-L-arabinofuranose (**1**) in aqueous solution.

conformers decreases with an increase in solvent polarity from 17.1 and 11.5% to 11.0 and 7.1% in water. This is counterbalanced by the increase of the C1 conformer; 64.8% in vacuum vs. 74.5% in water. The population of the remaining conformers is lower than 10% and does not change significantly with solvent.

Two main differences appear when comparing the solution behaviour of **2** with **1**. First, the distribution of conformers in the equilibrium mixture of **1** is more balanced; secondly, the populations of conformers in the equilibrium mixture of **2** are more sensitive to solvation. Whereas five conformers of **1** with populations larger than 5% are involved in the equilibrium (C1-N: C1-S: C2-S: C3-S: C3-N: C4-S: C5-S: C6-S: C6-N: C7-S: C7-N = 52.1 : 22.4 : 11.0 : 7.0 : 0.1 : 5.6 : 0.8 : 0.0 : 0.0 : 0.8 : 0.1) in aqueous solution, one conformer (P1-N) of **2** is dominant with the population higher then 85%. Based on the PCILO calculated energies, P1-N: P1-S: P2-S: P3-S: P3-N: P4-S: P5-S populations of 58.2 : 21.5 : 8.2 : 6.0 : 0.6 : 4.1 : 1.5 are predicted for **2** in a vacuum. A rather different distribution of P1-N: P1-S: P2-S: P3-S: P3-N: P4-S: P5-S = 85.2 : 3.3 : 2.7 : 2.9 : 0.8 : 4.5 : 0.5 was estimated for an aqueous solution of **2**.

The three staggered rotamers about the C-4–C-5 bond in **1** and **2**, denoted as *gg*, *gt*, and *tg* conformers, are present in the equilibrium. Minima with the *tg*

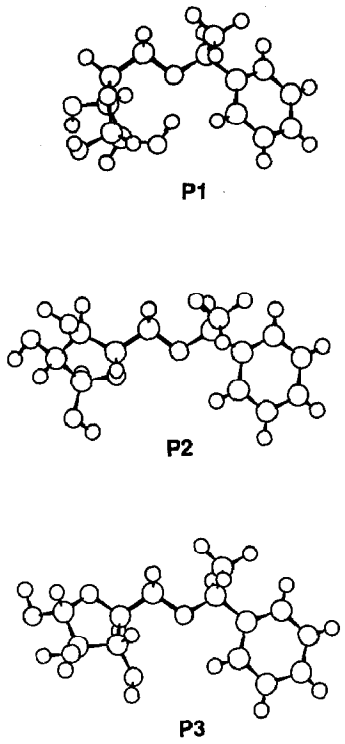

Fig. 4. Molecular representation of the three lowest energy conformations of 5-*O*-[(*S*)-1-phenethyl]-α-L-arabinofuranose (**2**) in aqueous solution.

orientation of the exocyclic group in **1** comprise five pseudorotamers (C3-S, C3-N, C5-S, C6-S, and C6-N), the minima with the *gt* orientation four (C1-N, C1-S, C7-S, and C7-N), and those with the *gg* orientation two pseudorotamers (C2-S and C4-S). For **2**, the *gt* orientation encloses two pseudorotamers (P1-N and P1-S), the *tg* orientation three (P3-S, P3-N, and P5-S), and the *gg* orientation two pseudorotamers (P2-S and P4-S). The calculated populations of (Ψ, ω) conformers can be used to estimate the distribution of conformers among the three stable staggered rotamers at C-4. The values in Tables 3 and 4 give *gg*: *gt*: *tg* populations in a vacuum of 22.2:65.2:12.6 for **1** and 12.3:79.7:8.0 for **2**. In aqueous solution, *gg* : *gt* : *tg* populations change to 16.6:75.4:8.0 for **1** and 7.2:88.5:4.3 for **2**. Thus, the population of the *gt* conformer in LCC appears to depend, in part, on the substituents at O-5, with larger values in the ether linkage than in the ester linkage.

The calculations on LCC models predict different relative populations of the three rotamers than those deduced from NMR measurements on arabinoxylan [19] and methyl α-L-arabinofuranoside [27]. Based on vicinal proton–proton coupling constants between H-4 and H-5 protons, relative populations of *gg* : *gt* : *tg* 37:46:17 in arabinoxylan [19] and 45:51:4 in methyl α-L-arabinofuranoside [27]

were estimated. A main difference is a larger population of *gt* rotamer and a lower population of *gg* rotamer in LCC models. However, in the *gg* and *gt* rotamers of arabinoxylan and methyl α-L-arabinofuranoside, an internal hydrogen bond can occur between HO-5 and the ring oxygen and these hydrogen bond interactions might have a different influence on the stabilisation of both rotamers. This stabilisation is not possible in LCC models because of the substituted HO-5 group. Moreover, in the *gt* rotamer, an intramolecular hydrogen bond can be formed between HO-2 and the exocyclic oxygen, but not in the *gg* rotamer. For example, for P1-N and C1-N conformers, the O-2–O-5 distance is 2.74 and 2.76 Å, respectively.

The superposition of the three most stable conformers for both LCC models shows interesting similarities in the overall shape of both molecules. Two different regions are clearly separated. The hydrophobic region, which consists of π-electrons of phenyl and carbonyl groups and lone-pairs of O-5; and the hydrophilic region, which consists of α-L-arabinofuranose hydroxyl groups. The hydrophobic and hydrophilic regions appear to be oriented perpendicularly to each other. Their mutual orientation is not influenced by the two main degrees of conformational freedom, which are the reorientation at C-4 and the pseudorotation of the ring. Thus, the overall shape of both compounds is determined mainly by the conformationally rigid linkage between the substituted benzene ring and O-5 of the α-L-arabinofuranose.

The coexistence of South and North conformations for the α-L-arabinofuranose ring present in wheat arabinoxylan [19] was proposed from the analysis of vicinal proton–proton coupling constants in aqueous solution. In this case, N- and S-type conformers are occupied in approximately equal amounts (N : S = 52 : 48). More recently, an investigation of the arabinofuranose ring conformational behaviour by means of the MM3 molecular mechanics method [27] stressed the importance of the substituents and the orientations at the C-1 and C-4 atoms on the conformational preference of the furanose ring. The solution conformations of the furanose ring are usually deduced from the vicinal $^1H–^1H$ coupling constants with the use of appropriate Karplus equations [28]. Experimental coupling constants $J_{1,2}$, $J_{2,3}$, and $J_{3,4}$ in the ranges 0.8–1.7, 2.3–3.2, and 5.0–5.8 Hz, respectively, were observed for a nonreducing residue [19,27] and values of 3.6, 6.0, and 7.0 Hz for a reducing residue [27]. These data represent time-average values and correspond, therefore, to the "virtual" conformation [29]. These results reflect the importance of the chemical structure for the conformational equilibrium of the furanose ring conformers and also imply that substitution at the anomeric centre shifts the equilibrium of ring pseudorotamers in the direction of N-type conformers.

In order to compare the calculated values for LCC models (**1** and **2**) with experimental data for the furanose residue in arabinoxylan, the three intraring $^3J_{H,H}$ constants were calculated for each minimum. The coupling constants were then averaged using their energies in aqueous solution. These calculated averages describe the "virtual" conformation in solution. The resulting values ($J_{1,2}$ 2.6, $J_{2,3}$ 3.1, and $J_{3,4}$ 4.3 Hz for **1**; and $J_{1,2}$ 1.5, $J_{2,3}$ 1.3, and $J_{3,4}$ 1.9 Hz for **2**) show that the "virtual" furanose ring conformation in these compounds is shifted in comparison

with that observed for a furanose residue in arabinoxylan. A comparison with corresponding average values calculated in a vacuum ($J_{1,2}$ 3.2, $J_{2,3}$ 4.0, and $J_{3,4}$ 5.5 Hz for **1**; and $J_{1,2}$ 2.2, $J_{2,3}$ 2.6, and $J_{3,4}$ 3.9 Hz for **2**) indicates that solvent effects change the "virtual" conformation of furanose rings in both compounds.

A more detailed picture of these changes can be seen from data given in Tables 3 and 4. A comparison of the populations shows that the conformational behaviour of the α-L-arabinofuranose ring of **1** differs from that of **2**. In a vacuum, the N- and S-type conformers of **1** are in the ratio 35:64 and S-type conformers are preferred. For **2**, this ratio is 59:41 and N-type conformers are more populated. The conformational equilibrium in both compounds is considerably influenced by solvent effects which induce an increase in the abundance of N-type ring conformers. This ratio is shifted in water to N:S = 53:47 for **1**. Thus, in aqueous solution, N-type conformers become slightly more populated. This ratio compares favourably with the N:S ratio of 52:48 observed in arabinoxylan [19]. For **2**, the preference of N-type conformers is even more enhanced and they are dominant species with a population larger than 86%.

4. Conclusions

The present work shows that the ester and ether linkages in lignin–carbohydrate complexes modelled by **1** and **2** display a large amount of conformational freedom. This involves a rapid equilibrium between various pseudorotamers of the furanose ring, rotamers of the exocyclic group, as well as rotation around the ester and ether linkages. The calculations indicate that the conformational behaviour of the α-L-arabinofuranose ring of **1** and **2** differs from that of methyl α-L-arabinofuranoside. In this case, the addition of the substituents to a furanose ring at O-5 reduces the conformational heterogeneity. Though both the North- and South-type conformers are likely to occur, the equilibrium in aqueous solution is considerably shifted to North conformers in the ether linkage model (**2**), whereas the N:S ratio in the ester linkage model (**1**) is comparable with the ratio in an arabinoxylan where they are almost equally populated. Furthermore, calculations indicate that the substitution also influences the equilibrium around the C-4–C-5 bond. In this case, the exocyclic group prefers the *gt* rotamer in both compounds. All the structural features described in the present work provide a basis for the generation of more accurate models for further studies of lignin–carbohydrate complexes.

References

[1] M. Remko, I. Tvaroska, M. Fiserová, and R. Brezny, *Z. Phys. Chem. (Leipzig)*, 271 (1990) 927–930.
[2] T. Koshijima, T. Taniguchi, and R. Tanaka, *Holzforschung*, 26 (1972) 211–217.
[3] M. Neilson and G.N. Richards, *Carbohydr. Res.*, 104 (1982) 121–138.
[4] T. Higuchi and Y. Nakamura, *Cellul. Chem. Technol.*, 12 (1978) 199–208.
[5] B. Kosíková, D. Joniak, and L. Kosáková, *Holzforschung*, 33 (1979) 11–14.
[6] G.J. Leary, D.A. Sawtell, and H. Wong, *Holzforschung*, 37 (1983) 11–16.

[7] T. Iversen and S. Wännström, *Holzforschung*, 40 (1986) 9–22.
[8] J.P. Joseleau and R. Kesraovi, *Holzforschung*, 40 (1986) 163–168.
[9] J.I. Azuma and T. Koshijima, *Methods Enzymol.*, 161 (1988) 12–18.
[10] B. Kosíková, J. Joniak, and J. Polcin, *Holzforschung*, 27 (1973) 56–64.
[11] N. Takahashi, J. Azuma, and T. Koshijima, *Carbohydr. Res.*, 107 (1982) 161–168.
[12] O. Erikson, D.A.J. Goring, and B.O. Lindgren, *Wood Sci. Technol.*, 14 (1980) 267–279.
[13] G.J. Leary, D.A. Sawtell, and H. Wong, *Holzforschung*, 37 (1983) 11–16.
[14] M. Remko, *Holzforschung*, 40 (1986) 205–209.
[15] T. Liptaj, M. Remko, and J. Polcin, *Collect. Czech. Chem. Commun.*, 45 (1980) 330–334.
[16] P. Diner, J.P. Malrieu, F. Jordan, and M. Gilbert, *Theor. Chim. Acta*, 15 (1969) 100–110.
[17] I. Tvaroska and T. Bleha, *Adv. Carbohydr. Chem. Biochem.*, 47 (1989) 45–123.
[18] D. Cremer and J.A. Pople, *J. Am. Chem. Soc.*, 97 (1975) 1354–1355.
[19] R.A. Hoffmann, J. van Wijk, B.R. Leeflang, J.P. Kamerling, C. Altona, and J.F.G. Vliegenthart, *J. Am. Chem. Soc.*, 114 (1992) 3710–3714.
[20] I.M. Piper, D.B. McLean, R. Faggiani, C.J.L. Lock, and W.A. Szarek, *Can. J. Chem.*, 63 (1985) 2915–2921.
[21] I.M. Piper, D.B. McLean, R. Faggiani, C.J.L. Lock, and W.A. Szarek, *Can. J. Chem.*, 63 (1985) 2913–2914.
[22] O. Lefebvre-Sonbeyran, C. Stora, and G. Barnathan, *Cryst. Struct. Commun.*, 5 (1976) 459–464.
[23] B.M. Goldstein, D.T. Mao, and V.E. Marquez, *J. Med. Chem.*, 31 (1988) 1026–1031.
[24] I. Tvaroska and T. Kozár, *J. Am. Chem. Soc.*, 102 (1980) 6929–6936.
[25] I. Tvaroska, *Biopolymers*, 21 (1982) 1887–1897.
[26] S. Wolfe, *Acc. Chem. Res.*, 5 (1972) 102–111.
[27] S. Cros, C. Hervé du Penhoat, S. Perez, and A. Imberty, *Carbohydr. Res.*, 248 (1993) 81–93.
[28] C.A.G. Haasnoot, F.A.A.M. De Leeuw, and C. Altona, *Tetrahedron*, 36 (1980) 2783–2792.
[29] O. Jardetzky, *Biochim. Biophys. Acta*, 621 (1980) 227–232.